Published in final edited form as:
Hum Genet. 2009 October ; 126(4): 589–602. doi:10.1007/s00439-009-0706-x.

Redefined genomic architecture in 15q24 directed by patient deletion/duplication breakpoint mapping

Ayman W. El-Hattab,
Department of Molecular and Human Genetics, Baylor College of Medicine, One Baylor Plaza, Rm R809, Houston, TX 77030, USA

Teresa A. Smolarek,
Division of Human Genetics, Cincinnati Children's Hospital Medical Center, Cincinnati, OH 45229, USA

Martha E. Walker,
Division of Human Genetics, Cincinnati Children's Hospital Medical Center, Cincinnati, OH 45229, USA

Elizabeth K. Schorry,
Division of Human Genetics, Cincinnati Children's Hospital Medical Center, Cincinnati, OH 45229, USA

LaDonna L. Immken,
Clinical Genetics, Specially for Children, Austin, TX 78723, USA

Gayle Patel,
Clinical Genetics, Specially for Children, Austin, TX 78723, USA

Mary-Alice Abbott,
Clinical Genetics, Baystate Medical Center, Springfield, MA 01199, USA

Brendan C. Lanpher,
Division of Genetics and Genomic Medicine, Vanderbilt University, Nashville, TN 37232, USA

Zhishuo Ou,
Department of Molecular and Human Genetics, Baylor College of Medicine, One Baylor Plaza, Rm R809, Houston, TX 77030, USA

Sung-Hae L. Kang,
Department of Molecular and Human Genetics, Baylor College of Medicine, One Baylor Plaza, Rm R809, Houston, TX 77030, USA

Ankita Patel,
Department of Molecular and Human Genetics, Baylor College of Medicine, One Baylor Plaza, Rm R809, Houston, TX 77030, USA

Fernando Scaglia,
Department of Molecular and Human Genetics, Baylor College of Medicine, One Baylor Plaza, Rm R809, Houston, TX 77030, USA

James R. Lupski,
Department of Molecular and Human Genetics, Baylor College of Medicine, One Baylor Plaza, Rm R809, Houston, TX 77030, USA

Correspondence to: Pawel Stankiewicz, pawels@bcm.edu.

Sau Wai Cheung, and
Department of Molecular and Human Genetics, Baylor College of Medicine, One Baylor Plaza, Rm R809, Houston, TX 77030, USA

Pawel Stankiewicz
Department of Molecular and Human Genetics, Baylor College of Medicine, One Baylor Plaza, Rm R809, Houston, TX 77030, USA

Department of Medical Genetics, Institute of Mother and Child, Warsaw, Poland

Pawel Stankiewicz: pawels@bcm.edu

Abstract

We report four new patients with a submicroscopic deletion in 15q24 manifesting developmental delay, short stature, hypotonia, digital abnormalities, joint laxity, genital abnormalities, and characteristic facial features. These clinical features are shared with six recently reported patients with a 15q24 microdeletion, supporting the notion that this is a recognizable syndrome. We describe a case of an ~2.6 Mb microduplication involving a portion of the minimal deletion critical region in a 15-year-old male with short stature, mild mental retardation, attention deficit hyperactivity disorder, Asperger syndrome, decreased joint mobility, digital abnormalities, and characteristic facial features. Some of these features are shared with a recently reported case with a 15q24 microduplication involving the minimal deletion critical region. We also report two siblings and their mother with duplication adjacent and distal to this region exhibiting mild developmental delay, hypotonia, tapering fingers, characteristic facial features, and prominent ears. The deletion and duplication breakpoints were mapped by array comparative genomic hybridization and the genomic structure in 15q24 was analyzed further. Surprisingly, in addition to the previously recognized three low-copy repeat clusters (BP1, BP2, and BP3), we identified two other paralogous low-copy repeat clusters that likely mediated the formation of alternative sized 15q24 genomic rearrangements via non-allelic homologous recombination.

Introduction

The recent expanded use of high resolution genome analysis by array comparative genomic hybridization (array CGH) has led to the identification of several novel microdeletion and microduplication syndromes (Slavotinek 2008; Stankiewicz and Beaudet 2007). These rearrangements can be recurrent, resulting from non-allelic homologous recombination (NAHR) between homologous low-copy repeats (LCRs), and lead to loss or gain of a dosage-sensitive gene or genes (Stankiewicz and Lupski 2002) like 15q13.3 deletion (Sharp et al. 2008), 15q24 deletion (Sharp et al. 2007), 17p11.2 deletion (Smith–Magenis syndrome) and duplication (Potocki–Lupski syndrome) (Bi et al. 2003; Potocki et al. 2007), and 17q21.31 deletion and duplication (Kirchhoff et al. 2007; Koolen et al. 2006; Sharp et al. 2006; Shaw-Smith et al. 2006). Recently, a number of non-recurrent rearrangements have been shown also to result from genomic architectural features that may stimulate their formation through the proposed fork stalling and template switching (FoSTeS)/microhomology-mediated break-induced replication (MMBIR) mechanism (Lee et al. 2007), e.g., *MECP2* duplication (Carvalho et al. 2009), deletions and duplications in 17p13.3 (Bi et al. 2009; Nagamani et al. 2009), and deletions and duplications in 17p11.2 (Zhang et al. 2009; for review see Gu et al. 2008).

With the exception of the common recurrent 15q11.2q12 deletions which, depending on parental origin, result in either Prader–Willi syndrome or Angelman syndrome, and deletions and duplications in 15q13.3 (Sharp et al. 2008; Ben-Shachar et al. 2009), rearrangements of chromosome 15q are relatively rare (Cushman et al. 2005); those

involving the 15q24 region were described in patients with growth deficiency, psychomotor retardation, and birth defects (Bettelheim et al. 1998; Clark 1984; Formiga et al. 1988; Spruijt et al. 2004). Cushman et al. (2005) reported three patients with a 15q24 deletion and reviewed the previously reported cases with cytogenetically visible deletions involving the 15q22q24 region. They concluded that the majority of these cases shared developmental delay, growth deficiency, hypotonia, skeletal abnormalities, urogenital system defects, and similar facial features, including epicanthal folds, ear abnormalities, and arched palate, and it was suggested that these cases represent a new cytogenetic deletion syndrome.

Sharp et al. (2007) identified overlapping submicroscopic 15q24 deletions in four patients with developmental delay, growth deficiency, digital abnormalities, hypospadias, loose connective tissue, and characteristic facial features, including high anterior hair line, broad medial eyebrows, hypertelorism, down-slanting palpebral fissures, long smooth philtrum, and full lower lip. The deletion breakpoints mapped to homologous LCR clusters, designated as BP1, BP2, and BP3, with a minimal deletion critical region of ~1.7 Mb spanning the genomic interval from BP1 to BP2. Subsequently, Klopocki et al. (2008) reported another patient who shared common clinical features with the previously reported patients and had a 15q24 microdeletion with breakpoints mapping to BP1 and BP3. Recently, Van Esch et al. (2009) described an additional patient with a 15q24 microdeletion, who presented with features common to the previously reported patients, including developmental delay, loose connective tissue, digital and genital anomalies, and distinct facial features; in addition, this patient has a congenital diaphragmatic hernia. The proximal deletion breakpoint mapped to an LCR cluster located proximal to BP1, whereas the distal breakpoint coincided with BP2.

Six cytogenetically visible interstitial duplications involving 15q24 have been reported in patients with growth deficiency, psychomotor retardation, birth defects, and characteristic facial features, including facial asymmetry, ear malformations, micrognathia and palatal clefting (Browne et al. 2000; Dhaliwal et al. 1990; Han et al. 1999; Roggenbuck et al. 2004). Pectus excavatum was found to be associated with a duplication in 15q23–q26 (Brewer et al. 1999). Recently, an ~1.7 Mb microduplication in 15q24, extending from BP1 to BP2, has been described in a 2-year-old boy with global developmental delay, characteristic facial features, digital and genital abnormalities. This duplication is apparently reciprocal to the minimal deletion critical region for the 15q24 deletion syndrome and was inherited from his healthy father (Kiholm Lund et al. 2008).

We report four new patients with an overlapping 15q24 microdeletion (cases 1–4) and further delineate the 15q24 deletion syndrome. In addition, we describe four patients with 15q24 microduplications: one patient (case 5) with duplication involving part of the minimal deletion critical region, and two siblings (cases 6 and 7) and their mother, who have duplication adjacent and distal to the minimal deletion critical region. We also redefine the genomic structure of this chromosomal region guided by breakpoint mapping of the above patients that revealed additional LCR clusters.

Subjects and methods

DNA samples

Patients 1–5 were referred to the Medical Genetics Laboratories of Baylor College of Medicine for clinical array-CGH analysis. Patients 6 and 7 were referred to the Cytogenetic Laboratory of Cincinnati Children's Hospital Medical Center for SNP array analysis. DNA samples were obtained from the probands and their family members after informed consents approved by the Institutional Review Board for Human Subject Research at Baylor College of Medicine or Cincinnati Children's Hospital Medical Center. DNA was extracted from

whole blood using the Puregene DNA extraction kit (Gentra, Minneapolis, MN, USA) according to the manufacturer's instructions.

Array CGH

The four 15q24 deletion cases 1–4 and the duplication case 5 were identified through screening the database of Baylor College of Medicine Medical Genetics Laboratories of array CGH studies performed in over 9,000 patients using oligonucleotide Chromosomal Microarray Analysis (CMA Versions 6 and 7 OLIGO) (Cheung et al. 2005; Ou et al. 2008). Of these patients, approximately 4,700 patients were tested using V6 OLIGO (44 K array) and over 4,000 patients using V7 OLIGO (105 K array).

The oligonucleotide based chromosomal microarray version 6 (CMA V6 OLIGO) consists of 44 K targeted oligonucleotides emulating genomic regions contained within BAC clones arranged in the BAC V6 CMA. It contains an average of 28–30 oligos per genomic region interrogated by single BAC clones with a minimum of approximately 10–15 oligos whenever possible (Ou et al. 2008). This array was used for patients 2, 3, and 4.

The oligonucleotide based chromosomal microarray version 7 (CMA V7 OLIGO) utilizes array-based comparative genomic hybridization with approximately 105,000 oligos covering the whole genome at an average resolution of 30 kb with increased coverage at known disease loci. Included in CMA are probes for all the known microdeletion/microduplication syndromes (over 270 genetic syndromes), 41 unique subtelomeric regions, all 43 unique pericentromeric regions and the mitochondrial genome. In addition to these targeted regions, the entire genome (between disease regions) is covered with an average resolution of 30 kb, excluding repetitive sequences through a combination of bioinformatics, computation, and empirical studies. The array also includes six regions of known polymorphic variants: the *Amylase* (*AMY1A*) gene cluster in lp21.2, the *UDP glucuronosyltransferase 2* (*UGT2B17*) *g*ene in 4q13.2, the *chemokine CC motif ligand 3 and 4* (*CCL3, CCL4*) genes in 17q12, the *defensin beta 107B* (*DEFB107B*) gene family in 8p23.1, the *opsin 1 medium-wave-sensitive 2* (*OPN1MW2*) gene in Xq28, and exon 2 of the *Apolipoprotien* (*LPA*) gene in 6q26 to serve as internal controls. This array was performed in patients 1 and 5. Patient 2 was also analyzed with CMA V.7 OLIGO to better delineate the breakpoints (Fig. 1a, b).

The rearrangements in three patients (cases 3–5) were further investigated using a high-resolution Agilent 244 K Whole Human Genome Oligo Microarray (Agilent Technologies, Inc., Santa Clara, CA), which contains 238,459 probes, representing a compiled view of the human genome at a 8.9 kb overall median probe spacing (7.4 kb in Refseq genes) (http://www.chem.agilent.com) (Fig. 1c). The procedures for DNA digestion, labeling, and hybridization were performed according to the manufacturer's instructions with some modifications (Probst et al. 2007).

The slides were scanned into image files using a GenePix Model 4000B microarray scanner (Molecular Devices, Sunnyvale, CA, USA) or an Agilent G2565 laser scanner. Microarray image files of oligo arrays were quantified using Agilent Feature extraction software (v9.0), and text file outputs from the quantitation analysis were imported to our in-house analysis package for copy number analysis, as described (Ou et al. 2008).

SNP microarray

SNP microarray studies were performed in patients 6 and 7 using the commercially available Illumina 370 K DNA Beadchip. DNA was processed according to manufacturer's specifications and chips processed according to the protocol.

Cytogenetic and FISH analyses

Confirmatory chromosome and FISH analyses with BAC clones were performed on peripheral blood lymphocytes using standard procedures after detection of copy number changes observed in the CMA as described by Shchelochkov et al. (2008).

Bioinformatics and in silico sequence analysis

Genomic sequence based on the oligonucleotide coordinates from the array CGH experiment was downloaded from UCSC genome browser (Build 36, UCSC genome browser, March 2006). Interspersed repeat sequences were analyzed by RepeatMasker (http://www.repeatmasker.org). Regional assemblies for known LCR15q24s (BP1, BP2, and BP3) and a search for additional LCRs were assembled using NCBI BLAST 2 and the Sequencher software (Gene Codes). We eliminated small insertions/deletions from the calculation of the DNA sequence identity and took only base pair changes into account.

Results

Clinical findings associated with 15q24 deletion and duplication

We identified overlapping 15q24 microdeletions involving the minimal critical region and ranging in size from 3.10 to 3.95 Mb, in four unrelated patients (cases 1–4). These individuals share many features, including developmental delay, short stature, hypotonia, digital anomalies, joint laxity, genital abnormalities, and characteristic facial features, including a long smooth philtrum and ear malformations (Table 1; Fig. 2a, b). The deletions are de novo in patients 1, 3, and 4. The mother of patient 2 was reported to be healthy, but limited data are available about the father, and both parents were not tested.

We also identified four patients with a 15q24 microduplication, one patient (case 5) has a duplication involving a portion of the minimal deletion critical region, whereas two siblings (case 6–7) and their mother have a duplication adjacent and distal to the minimal deletion critical region. Patient 5 is a 15-year-old male with short stature, mild mental retardation (IQ 71), behavioral problems, decreased range of motion of elbows, wrist and fingers, increased tone, and characteristic facial features (Table 2; Fig. 2c). Serum amino acids and urine organic acid analysis, karyotype, fragile X syndrome DNA testing, brain MRI, and EEG were all normal. Chromosomal microarray analysis revealed an ~ 2.62 Mb duplication in 15q24 (70.708–73.332 Mb, build 36). The mother was reported to have depression. She was tested by FISH for the duplication with normal results. The father was reported to have schizophrenia; he was not available for either examination or testing, but the mother reported that the patient's facial features do not resemble his father's facies.

Patient 6 is a 3.5-year-old boy with mild global developmental delay, truncal hypotonia, lower extremity hypertonia, and characteristic facial features (Table 2; Fig. 2d). Renal ultrasound, brain MRI, hearing evaluation, fragile X syndrome DNA testing, and karyotype all were normal. A SNP microarray revealed an ~2.11 Mb duplication of chromosome 15q24 (73858160–75969880, build 36). His 2-year-old sister (case 7) has developmental delay, truncal hypotonia, and characteristic facial features (Table 2). SNP microarray revealed the same ~2.11 Mb duplication in chromosome 15q24. Both children were adopted. The biological mother, who has been described as a slow learner and attended special education classes in school, was tested by FISH and found to have the same duplication; she was unavailable for physical examination, and limited data were available about her medical and mental history (Table 2). Both the sister (case 7) and the mother were also found to have gain of 15 clones at Xp22.31 that was interpreted as a benign copy number change.

Additional complexity to 15q24 genomic architecture

Using Blast2, we analyzed the DNA sequence in the 15q24 region between 70.600 and 76.600 Mb that harbors all the genomic rearrangements, and searched for alignments more than 300 bp in length and greater than 90% DNA sequence identity. Unexpectedly, in addition to the three previously identified LCR clusters (BP1, BP2, and BP3) (Sharp et al. 2007), we identified two more paralogous LCR clusters that we designated LCR15q24A, spanning ~65 kb, and located proximal to BP1, and LCR15q24C, spanning ~ 124 kb, and located between BP1 and BP2. For consistency, we elected to change the nomenclature for the previously identified LCR clusters as follows: LCR15q24B for BP1 (spanning ~54 kb), LCR15q24D for BP2 (spanning ~ 128 kb), and LCR15q24E for BP3 (spanning ~93 kb). We constructed a physical map for this region where LCR subunits with identity greater than 90% are represented with the similar-colored arrows with arrowheads indicating the LCR subunit orientations and arrows lengths, the subunit sizes. Most of these subunits have DNA sequence identity greater than 95% and are represented in darker colors (e.g. red), whereas some subunits have sequence identity between 90 and 94%, and those subunits are shown in lighter colors (e.g. light red) (Fig. 3; Table 3). Interestingly, the homologous subunits located in LCR15q24A and LCR15q24C are in direct orientation, whereas the subunits located in LCR15q24B (BP1) and LCR15q24E (BP3) are in the opposite orientation to the subunits located in LCR15q24A and LCR15q24C. In contrast, LCR15q24D (BP2) has a complex structure with most of the subunits being directly oriented with reference to LCR15q24A and LCR15q24C, whereas two small sub-units (~3 kb subunit in light green color and ~7 kb subunit in light brown color as shown in Fig. 3) are directly oriented to subunits in LCR15q24B and LCR15q24E.

Rearrangement breakpoint analysis supports genomic complexity

The breakpoints for the deleted and the duplicated regions were determined using either array CGH or SNP arrays. The proximal and distal deletion breakpoints in patients 1 and 2 map to LCR15q24B (BP1) and LCR15q24E (BP3), respectively. The proximal breakpoints for the deletions in patients 3 and 4, and the duplication in patient 5, map to LCR15q24A. The distal breakpoints for deletions in patients 3 and 4 map to LCR15q24D (BP2); however, the distal breakpoint for duplication in patient 5 maps to the novel LCR15q24C. The proximal and distal breakpoints for duplications in patients 6 and 7 map to LCR15q24D (BP2) and LCR15q24E (BP3), respectively (Fig. 4). The findings of breakpoints mapping to LCRs support that NAHR is the mechanism for these alterations.

Discussion

By comparing the clinical features in our four 15q24 microdeletion patients (cases 1–4) with the other six previously reported patients with a 15q24 microdeletion (Klopocki et al. 2008; Sharp et al. 2007; Van Esch et al. 2009), we observed many common features, supporting the notion that subjects harboring 15q24 deletion manifest a distinct syndrome (Table 1, Table 2). These features include developmental delay that varies from mild to severe, hypotonia, short stature, digital anomalies, joint laxity, genital anomalies, and characteristic facial features, including a high anterior hair line, facial asymmetry, ear malformations, broad medial eyebrows, down-slanted palpebral fissures, hypertelorism, epicanthal folds, strabismus, long smooth philtrum, full lower lip, and broad nasal base. The distal extremity malformations observed in all reported patients consist of thumb anomalies, small hands with brachydactyly, clinodactyly, and foot-ankle deformities. Less common features are microcephaly, IUGR, feeding difficulties, low tone or nasal speech, and obesity. Diaphragmatic hernia was observed in two patients (Sharp et al. 2007; Van Esch et al. 2009); tetralogy of Fallot and myelomeningocele were observed in one patient (case 2), and acute lymphoblastic leukemia was also found in one patient (case 1). All patients with a

15q24 microdeletion share the same ~ 1.75 Mb minimal deletion critical region located between LCR15q24B (BP1) and LCR15q24D (BP2) (Fig. 4).

Recently, a microduplication in 15q24 involving the minimal critical deletion region has been described with proximal and distal breakpoints mapping to LCR15q24B (BP1) and LCR15q24D (BP2), respectively (Kiholm Lund et al. 2008). We identified another case of a 15q24 microduplication involving a portion of the minimal deletion critical region, mapping from LCR15q24A to LCR15q24C (case 5) (Fig. 4). These two patients share some clinical features, including developmental delay, hypertonia, joints limitation, digital abnormalities, and certain facial features, including down-slanting palpebral fissures, epicanthus, full eyelids, smooth philtrum, and full lower lip. The previously reported patient with a 15q24 microduplication had hypospadias, agenesis of corpus callosum, low set ears, and normal growth parameters; however, our patient has normal genitalia, normal brain MRI, normally set ears, short stature, and behavioral problems (Table 2). These two patients with a 15q24 duplication involving the minimal critical deletion region share some overlapping features with patients with a 15q24 deletion, including developmental delay, short stature, digital anomalies, genital anomalies and some facial features (epicanthal folds, down-slanting palpebral fissures, hypertelorism, ear malformation, smooth philtrum, and full lower lip). Most patients with a 15q24 deletion have hypotonia and joint laxity, whereas the two patients with duplication exhibit increased tone and joints limitations. Patient 5 exhibits behavioral disorders that were not reported in patients with the 15q24 deletion syndrome (Table 2). The patient reported by Kiholm Lund et al. (2008) inherited the duplication from a healthy father; the father of patient 5 was unavailable for testing, so it is unclear whether the duplications are responsible for the observed phenotype. However, the similarity in the phenotype between these two patients and the overlapping features with patients with 15q24 deletion support the contention that this duplication could be responsible for the observed phenotype, suggesting that a 15q24 duplication may represent a clinical syndrome with minimal critical region of 1.33 Mb spanning between LCR15q24B (BP1) and LCR15q24C (Fig. 4). Nevertheless, more subjects with similar duplications need to be studied to support or refute this hypothesis.

We also report two siblings and their mother with a 15q24 microduplication distal and adjacent to the minimal deletion critical region with breakpoints mapping to LCR15q24D (BP2) and LCR15q24E (BP3) (cases 6 and 7) (Fig. 4). These siblings manifest a milder phenotype with mild developmental delay, hypotonia, tapering fingers, and characteristic facial features, including round face, hypertelorism, and prominent ears (Table 2). The overlapping features between these siblings and patients with a 15q24 deletion are less obvious and include only developmental delay, hypotonia, and hypertelorism. The two siblings inherited the duplication from their mother; thus it is also unclear whether this duplication is responsible for the phenotype. However, the fact that their mother has learning disabilities and the similarity in the phenotype between the siblings indicate that this duplication could be responsible for the observed phenotype; nevertheless, more subjects with similar duplication need to be studied.

The finding of 15q24 deletion and duplication breakpoints clustering in LCR regions supports the notion that NAHR is the most likely mechanism for these genomic rearrangements (Stankiewicz and Lupski 2002). LCR15q24B (BP1) and LCR15q24E (BP3) contain multiple homologous sub-units that are directly oriented and they harbor breakpoints for the deletions in patients 1 and 2. In addition, LCR15q24A and LCR15q24C contain multiple homologous subunits that are directly oriented and they encompass breakpoints of the duplication in patient 5. The proximal breakpoints for duplications in patients 6 and 7, and the distal breakpoints for deletions in patients 3 and 4 map to LCR15q24D (BP2) that has a complex structure with most subunits being directly oriented to LCR15q24A. The

latter repeat harbors the proximal breakpoints for deletions in patients 3 and 4. LCR15q24D (BP2) has two small subunits (~3 kb subunit in light green color and ~ 7 kb subunit in light brown color) directly oriented to subunits in LCR15q24E (BP3), that harbors the distal breakpoints for duplication in patients 6 and 7. These two small subunits are also directly oriented to the subunits inLCR15q24B (BP1). We therefore believe that these two small subunits mediated the NAHR in patients 6 and 7 and in patient ID204 (Sharp et al. 2007), who has a deletion with breakpoints mapping to 15q24B (BP1) and 15q24D (BP2) (Fig. 3, Fig. 4).

The four 15q24 deletion patients (cases 1–4) share the same 1.7 Mb minimal deletion region extending from LCR15q24B (BP1) to LCR15q24D (BP2). The deleted regions extend more distally in patients 1 and 2, the cases IMR349 and C45/06 (Sharp et al. 2007), and the case reported by Klopocki et al. (2008); compared to patients 3 and 4, case IMR371 (Sharp et al. 2007), and the case reported by Van Esch et al. (2009) with deletions extend more proximally (Fig. 4). Although all these patients share many similar features, they also differ in several aspects, e.g., growth deficiency and obesity (Table 1), and thus it is difficult to find a specific genomotype-phenotype (Bi et al. 2009) correlation with this limited set of patients for each specific deletion.

The critical region contains the *STRA6* gene that recently has been shown to be associated with syndromic microphthalmia, alveolar capillary dysplasia, and other malformations (Pasutto et al. 2007), the *cholesterol side chain cleavage enzyme* gene (*CYP11A1*) associated with lipoid congenital adrenal hyperplasia (Tajima et al. 2001), and the *mannose phosphate isomerase* gene (*MPI*) that is associated with congenital disorder of glycosylation type Ib (Niehues et al. 1998). All these disorders are autosomal recessive. It was suggested that the haploinsufficiency of cholesterol side chain cleavage enzyme might contribute to the genital abnormalities (Klopocki et al. 2008). There are two other candidate genes located in this region, which are related to the nervous system and their loss may contribute to the developmental delay. Semaphorin 7A (*SEMA7A*) enhances central and peripheral axon growth and is required for proper axon tract formation during embryonic development (Pasterkamp et al. 2007), and complexin 3 (*CPLX3*) is a positive regulator of neurotransmitter release in mouse hippocampal neurons (Reim et al. 2005) (Fig. 4).

Patient 1 developed acute lymphoblastic leukemia. The loss of two genes, *SIN3A* and *CSK*, may lead to an increased risk of developing neoplasm. *SIN3A* encodes a protein that participates in the formation of the histone deacetylase complex, which in turn interacts with tumor suppressor proteins like P53 and pRb (Fleischer et al. 2003). Cytoplasmic-src tyrosine kinase (*CSK*) down-regulates tyrosine kinase activity of the SRC oncoprotein and might function as an antioncogene (Armstrong et al. 1993) (Fig. 4). Larger numbers of patients with 15q24 deletion need to be studied before drawing any conclusions about neoplasm predisposition.

In conclusion, patients with a 15q24 deletion sharing the minimal deletion critical region between 15q24B (BP1) and 15q24D (BP2) have many common clinical features, supporting the notion that 15q24 deletion leads to a recognizable syndrome. Based on two patients with overlapping duplications, we better defined the phenotype of 15q24 duplication syndrome and narrowed its minimal critical region to ~1.3 Mb spanning between LCR15q24B (BP1) and the identified LCR15q24C. The breakpoints for the deleted and duplicated regions (except the case IMR371 (Sharp et al. 2007)) map to LCR clusters, indicating that NAHR is the likely mechanism of their formation.

Acknowledgments

We would like to thank our patients and their families. P.S. was supported in part by Grant R13-0005-04/2008 from the Polish Ministry of Science and Higher Education.

References

Armstrong E, Cannizzaro L, Bergman M, Huebner K, Alitalo K. The c-src tyrosine kinase (*CSK*) gene, a potential antioncogene, localizes to human chromosome region 15q23–q25. Cytogenet Cell Genet. 1993; 60:119–120. [PubMed: 1377109]

Ben-Shachar S, Lanpher B, German JR, Potocki L, Sreenath Nagamani SC, Franco LM, Malphrus A, Bottenfield GW, Spence JE, Amato S, Rousseau JA, Moghaddam B, Skinner C, Skinner SA, Bernes S, Armstrong N, Shinawi M, Stankiewicz P, Patel A, Cheung S-W, Lupski JR, Beaudet Al, Sahoo T. Microdeletion 15q13.3: a locus with incomplete penetrance for autism, mental retardation, and psychiatric disorders. J Med Genet. 2009; 46:382–388. [PubMed: 19289393]

Bettelheim D, Hengstaschlager M, Drhonsky R, Eppel W, Bernaschek G. Two cases of prenatally diagnosed diaphragmatic hernia accompanied by the same undescribed chromosomal deletion (15q24 de novo). Clin Genet. 1998; 53:319–320. [PubMed: 9650775]

Bi W, Park SS, Shaw CJ, Withers MA, Patel PI, Lupski JR. Reciprocal crossovers and a positional preference for strand exchange in recombination events resulting in deletion or duplication of chromosome 17p11.2. Am J Hum Genet. 2003; 73:1302–1315. [PubMed: 14639526]

Bi W, Sapir T, Shchelochkov OA, Zhang F, Withers MA, Hunter JV, Levy T, Shinder V, Peiffer DA, Gunderson KL, Nezarati MM, Shotts VA, Amato SS, Savage SK, Harris DJ, Day-Salvatore DL, Horner M, Lu XY, Sahoo T, Yanagawa Y, Beaudet AL, Cheung SW, Martinez S, Lupski JR, Reiner O. Increased LIS1 expression affects human and mouse brain development. Nat Genet. 2009; 41:168–177. [PubMed: 19136950]

Brewer C, Holloway S, Zawalnyski P, Schinzel A, FitzPatrick D. A chromosomal duplication map of malformations: regions of suspected haplo- and triplolethality—and tolerance of segmental aneuploidy—in humans. Am J Hum Genet. 1999; 64:1702–1708. [PubMed: 10330358]

Browne CE, Hatchwell E, Protopapas A, Ramos J. Duplication of medial 15q confirmed by FISH. J Med Genet. 2000; 37:E10. [PubMed: 10922390]

Carvalho CM, Zhang F, Liu P, Patel A, Sahoo T, Bacino CA, Shaw C, Peacock S, Pursley A, Tavyev YJ, Ramocki MB, Nawara M, Obersztyn E, Vianna-Morgante AM, Stankiewicz P, Zoghbi HY, Cheung SW, Lupski JR. Complex rearrangements in patients with duplications of *MECP2* can occur by Fork stalling and template switching. Hum Mol Genet. 2009; 18:2188–2203. [PubMed: 19324899]

Cheung SW, Shaw CA, Yu W, Li J, Ou Z, Patel A, Yatsenko SA, Cooper ML, Furman P, Stankiewicz P, Lupski JR, Chinault AC, Beaudet AL. Development and validation of a CGH microarray for clinical cytogenetic diagnosis. Genet Med. 2005; 7:422–432. [PubMed: 16024975]

Clark RD. Letter to the editor: del(15)(q22q24) syndrome with Potter sequence. Am J Med Genet. 1984; 19:703–705. [PubMed: 6517095]

Cushman LJ, Torres-Martinez W, Cherry AM, Manning MA, Abdul-Rahman O, Anderson CE, Punnett HH, Thurston VC, Sweeney D, Vance GH. A report of three patients with an interstitial deletion of chromosome 15q24. Am J Med Genet. 2005; 137:65–71. [PubMed: 16007617]

Dhaliwal MK, Menos D, Checkley P, Lieber E. A case of an unbalanced interstitial translocation involving chromosome 4p and 15q in a newborn with multiple congenital anomalies. Am J Hum Genet. 1990; 47(Suppl):A28.

Fleischer TC, Yun UJ, Ayer DE. Identification and characterization of three new components of the mSin3A corepressor complex. Mol Cell Biol. 2003; 23:3456–3467. [PubMed: 12724404]

Formiga LF, Poenaru L, Couronne F, Flori E, Eibel JL, Deminatti MM, Savary JB, Lai JL, Gilgenkrantz S, Pierson M. Interstitial deletion of chromosome 15: two cases. Hum Genet. 1988; 80:401–404. [PubMed: 3198122]

Gu W, Zhang F, Lupski JR. Mechanisms for human genomic rearrangements. Pathogenetics. 2008; 1:4. [PubMed: 19014668]

Han JY, Kim KH, Lee HD, Moon SY, Shaffer LG. De novo direct duplication of 15q15 → q24 in a newborn boy with mild manifestations. Am J Med Genet. 1999; 87:395–398. [PubMed: 10594877]

Kiholm Lund AB, Hove HD, Kirchhoff M. A 15q24 microduplication, reciprocal to the recently described 15q24 microdeletion, in a boy sharing clinical features with 15q24 microdeletion syndrome patients. Eur J Med Genet. 2008; 51:520–526. [PubMed: 18755302]

Kirchhoff M, Bisgaard AM, Duno M, Hansen FJ, Schwartz M. A 17q21.31 microduplication, reciprocal to the newly described 17q21.31 microdeletion, in a girl with severe psychomotor developmental delay and dysmorphic craniofacial features. Eur J Med Genet. 2007; 50:256–263. [PubMed: 17576104]

Klopocki E, Graul-Neumann LM, Grieben U, Tonnies H, Ropers HH, Horn D, Mundlos S, Ullmann R. A further case of the recurrent 15q24 microdeletion syndrome, detected by array CGH. Eur J Pediatr. 2008; 167:903–908. [PubMed: 17932688]

Koolen DA, Vissers LE, Pfundt R, de Leeuw N, Knight SJ, Regan R, Kooy RF, Reyniers E, Romano C, Fichera M, Schinzel A, Baumer A, Anderlid BM, Schoumans J, Knoers NV, van Kessel AG, Sistermans EA, Veltman JA, Brunner HG, de Vries BB. A new chromosome 17q21.31 microdeletion syndrome associated with a common inversion polymorphism. Nat Genet. 2006; 38:999–1001. [PubMed: 16906164]

Lee JA, Carvalho CM, Lupski JR. A DNA replication mechanism for generating nonrecurrent rearrangements associated with genomic disorders. Cell. 2007; 28:1235–1247. [PubMed: 18160035]

Nagamani SC, Zhang F, Shchelochkov OA, Bi W, Ou Z, Scaglia F, Probst FJ, Shinawi M, Eng C, Hunter JV, Sparagana S, Lagoe E, Fong CT, Pearson M, Doco-Fenzy M, Landais E, Mozelle M, Chinault AC, Patel A, Bacino CA, Sahoo T, Kang SH, Cheung SW, Lupski JR, Stankiewicz P. Microdeletions including *YWHAE* in the Miller-Dieker syndrome region on chromosome 17p13.3 result in facial dysmorphisms, growth restriction, and cognitive impairment. J Med Genet. 2009 (in press).

Niehues R, Hasilik M, Alton G, Körner C, Schiebe-Sukumar M, Koch HG, Zimmer KP, Wu R, Harms E, Reiter K, von Figura K, Freeze HH, Harms HK, Marquardt T. Carbohydrate-deficient glycoprotein syndrome type Ib: phosphomannose isomerase deficiency and mannose therapy. J Clin Invest. 1998; 101:1414–1420. [PubMed: 9525984]

Ou Z, Kang SH, Shaw CA, Carmack CE, White LD, Patel A, Beaudet AL, Cheung SW, Chinault AC, et al. Bacterial artificial chromosome-emulation oligonucleotide arrays for targeted clinical array-comparative genomic hybridization analyses. Genet Med. 2008; 10:278–289. [PubMed: 18414211]

Pasterkamp RJ, Peschon JJ, Spriggs MK, Kolodkin AL. Semaphorin 7A promotes axon outgrowth through integrins and MAPKs. Nature. 2007; 424:398–105. [PubMed: 12879062]

Pasutto F, Sticht H, Hammersen G, Gillessen-Kaesbach G, Fitzpatrick DR, Nürnberg G, Brasch F, Schirmer-Zimmermann H, Tolmie JL, Chitayat D, Houge G, Fernández-Martínez L, Keating S, Mortier G, Hennekam RC, von der Wense A, Slavotinek A, Meinecke P, Bitoun P, Becker C, Nürnberg P, Reis A, Rauch A. Mutations in *STRA6* cause a broad spectrum of malformations including anophthalmia, congenital heart defects, diaphragmatic hernia, alveolar capillary dysplasia, lung hypoplasia, and mental retardation. Am J Hum Genet. 2007; 80:550–560. [PubMed: 17273977]

Potocki L, Bi W, Treadwell-Deering D, Carvalho CM, Eifert A, Friedman EM, Glaze D, Krull K, Lee JA, Lewis RA, Mendoza-Londono R, Robbins-Furman P, Shaw C, Shi X, Weissenberger G, Withers M, Yatsenko SA, Zackai EH, Stankiewicz P, Lupski JR. Characterization of Potocki-Lupski syndrome (dup(17)(pll.2pll.2)) and delineation of a dosage-sensitive critical interval that can convey an autism phenotype. Am J Hum Genet. 2007; 80:633–649. [PubMed: 17357070]

Probst FJ, Roeder ER, Enciso VB, Ou Z, Cooper ML, Eng P, Li J, Gu Y, Stratton RF, Chinault AC, Shaw CA, Sutton VR, Cheung SW, Nelson DL. Chromosomal microarray analysis (CMA) detects a large X chromosome deletion including *FMR1, FMR2*, and *IDS* in a female patient with mental retardation. Am J Med Genet. 2007; 143A:1358–1365. [PubMed: 17506108]

Reim K, Wegmeyer H, Brandstatter JH, Xue M, Rosenmund C, Drebach T, Hofmann K, Brose N. Structurally and functionally unique complexins at retinal ribbon synapses. J Cell Biol. 2005; 69:669–680. [PubMed: 15911881]

Roggenbuck JA, Mendelsohn NJ, Tenenholz B, Ladda RL, Fink JM. Duplication of the distal long arm of chromosome 15: report of three new patients and review of the literature. Am J Med Genet. 2004; 126A:398–402. [PubMed: 15098238]

Sharp AJ, Hansen S, Selzer RR, Cheng Z, Regan R, Hurst JA, Stewart H, Price SM, Blair E, Hennekam RC, Fitzpatrick CA, Segraves R, Richmond TA, Guiver C, Albertson DG, Pinkel D, Eis PS, Schwartz S, Knight SJ, Eichler EE. Discovery of previously unidentified genomic disorders from the duplication architecture of the human genome. Nat Genet. 2006; 38:1038–1042. [PubMed: 16906162]

Sharp AJ, Selzer RR, Veltman JA, Gimelli S, Gimelli G, Striano P, Coppola A, Regan R, Price SM, Knoers NV, Eis PS, Brunner HG, Hennekam RC, Knight SJ, de Vries BB, Zuffardi O, Eichler EE. Characterization of a recurrent 15q24 microdeletion syndrome. Hum Mol Genet. 2007; 16:567–572. [PubMed: 17360722]

Sharp AJ, Mefford HC, Li K, Baker C, Skinner C, Stevenson RE, Schroer RJ, Novara F, De Gregori M, Ciccone R, Broomer A, Casuga I, Wang Y, Xiao C, Barbacioru C, Gimelli G, Bernardina BD, Torniero C, Giorda R, Regan R, Murday V, Mansour S, Fichera M, Castiglia L, Failla P, Ventura M, Jiang Z, Cooper GM, Knight SJ, Romano C, Zuffardi O, Chen C, Schwartz CE, Eichler EE. A recurrent 15q13.3 microdeletion syndrome associated with mental retardation and seizures. Nat Genet. 2008; 40:322–328. [PubMed: 18278044]

Shaw-Smith C, Pittman AM, Willatt L, Martin H, Rickman L, Gribble S, Curley R, Cumming S, Dunn C, Kalaitzopoulos D, Porter K, Prigmore E, Krepischi-Santos AC, Varela MC, Koiffmann CP, Lees AJ, Rosenberg C, Firth HV, de Silva R, Carter NP. Microdeletion encompassing *MAPT* at chromosome 17q21.3 is associated with developmental delay and learning disability. Nat Genet. 2006; 38:1032–1037. [PubMed: 16906163]

Shchelochkov OA, Cooper ML, Ou Z, Peacock S, Yatsenko SA, Brown CW, Fang P, Stankiewicz P, Cheung SW. Mosaicism for r(X) and der(X)del(X)(pll.23)dup(X) (pll.21pll.22) provides insight into the possible mechanism of rearrangement. Mol Cytogenet. 2008; 1:16. [PubMed: 18655707]

Slavotinek AM. Novel microdeletion syndromes detected by chromosome microarrays. Hum Genet. 2008; 124:1–17. [PubMed: 18512078]

Spruijt L, Engelen JJM, Bruinen-Smeijsters LP, Albrechts JCM, Schrander J, Schrander-Stumpel CTRM. A patient with a de novo 15q24q26.1 interstitial deletion, developmental delay, mild dysmorphism and very blue irises. Am J Med Genet. 2004; 129A:312–315. [PubMed: 15326635]

Stankiewicz P, Beaudet AL. Use of array CGH in the evaluation of dysmorphology, malformations, developmental delay, and idiopathic mental retardation. Curr Opin Genet Dev. 2007; 17:182–192. [PubMed: 17467974]

Stankiewicz P, Lupski JR. Genome architecture, rearrangements and genomic disorders. Trends Genet. 2002; 18:74–82. [PubMed: 11818139]

Tajima T, Fujieda K, Kouda N, Nakae J, Miller WL. Heterozygous mutation in the cholesterol side chain cleavage enzyme (P450scc) gene in a patient with 46, XY sex reversal and adrenal insufficiency. J Clin Endocr Metab. 2001; 86:3820–3825. [PubMed: 11502818]

Van Esch H, Backx L, Pijkels E, Fryns JP. Congenital diaphragmatic hernia is part of the new 15q24 microdeletion syndrome. Eur J Med Genet. 2009; 52:153–156. [PubMed: 19233321]

Zhang F, Khajavi M, Connolly AM, Towne CF, Batish SD, Lupski JR. The DNA replication FoSTeS/MMBIR mechanism can generate human genomic, genic, and exonic complex rearrangements. Nat Genet. 2009 (in press).

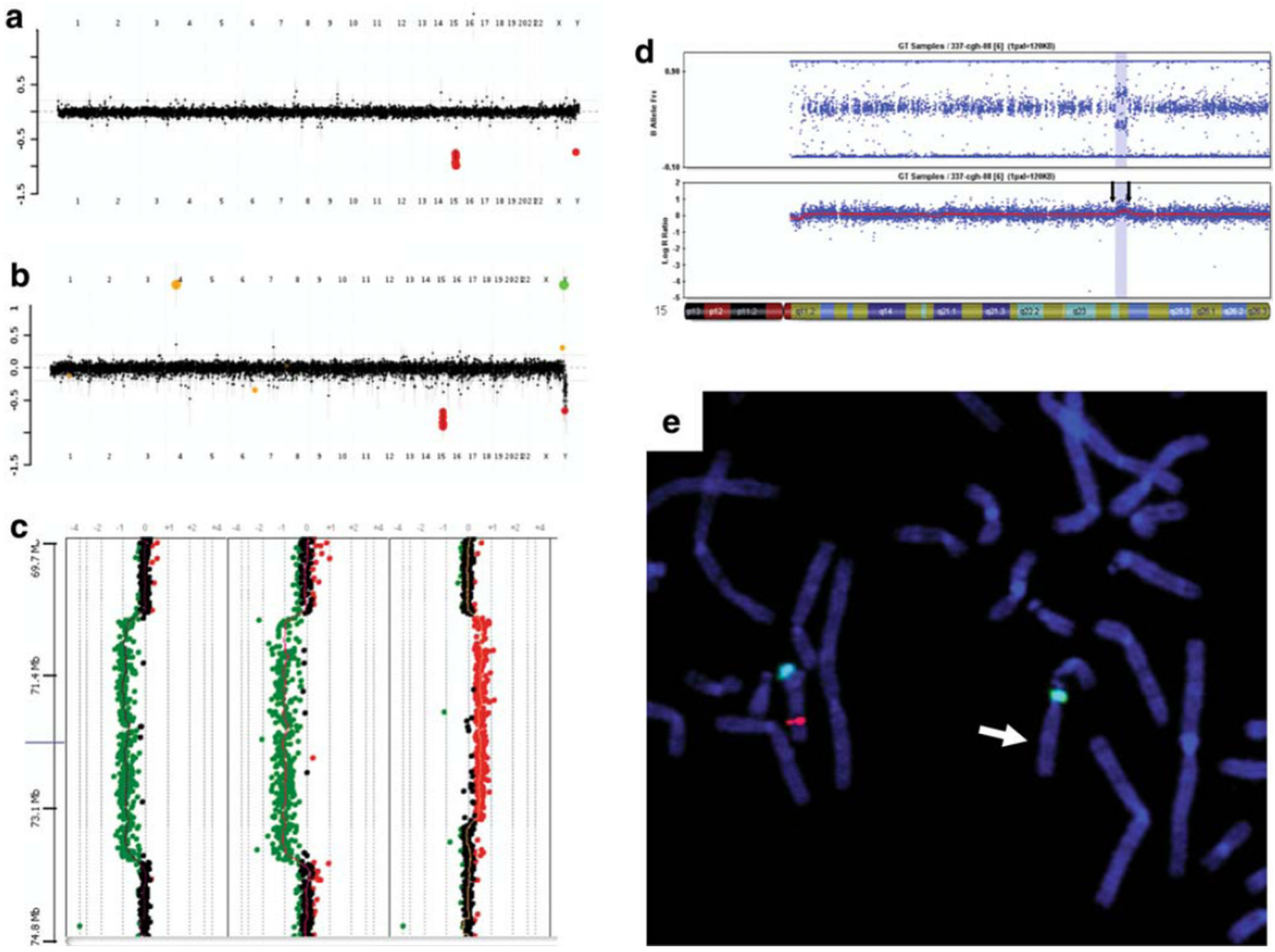

Fig. 1.

a, b The oligonucleotide based chromosomal microarray version 7 (CMA V7 OLIGO) profiles for patients 1 and 2. The averaged combined data of hybridizations performed using reference DNA. Oligonucleotides presented with *red color* and displaced down, indicating a loss of chromosome 15 material in the patient versus the reference DNA. c Results of Agilent 244 K array-based oligonucleotide CGH performed on DNA samples for patients 3 showing the deleted region 15q24 (70.750–73.856 Mb), patient 4 showing the deleted region (70.780–73.856 Mb), and patient 5 showing the duplicated region 15q24 (70.708–73.332 Mb). A deviation of the dots to the left of the central axis indicates a loss in copy number (represented with *green dots*), and a deviation to the right of the central axis indicates a gain in copy number (represented by *red dots*). **d** Chromosome 15q24 duplication in patients 6 and 7 using the Illumina DNA Beadarray (SNP) 370 K chip (region indicated by *arrows* and shaded). The *upper plot* shows the B allele frequency and the *lower plot* shows the Log R ratio (DNA dosage). SNP region is showing duplication between rs9672824 and rs4886534. Linear position on chromosome 15:73858160–75969880, with the total size of 2.11 Mb, and including 208 markers. **e** Results of the FISH analysis in patient 4. The *two green fluorescence signals* represent chromosome 15 centromeric FISH probe, and the *single red signal* represents probe specific to the deleted region (indicated by *arrow*), confirming the 15q24 deletion

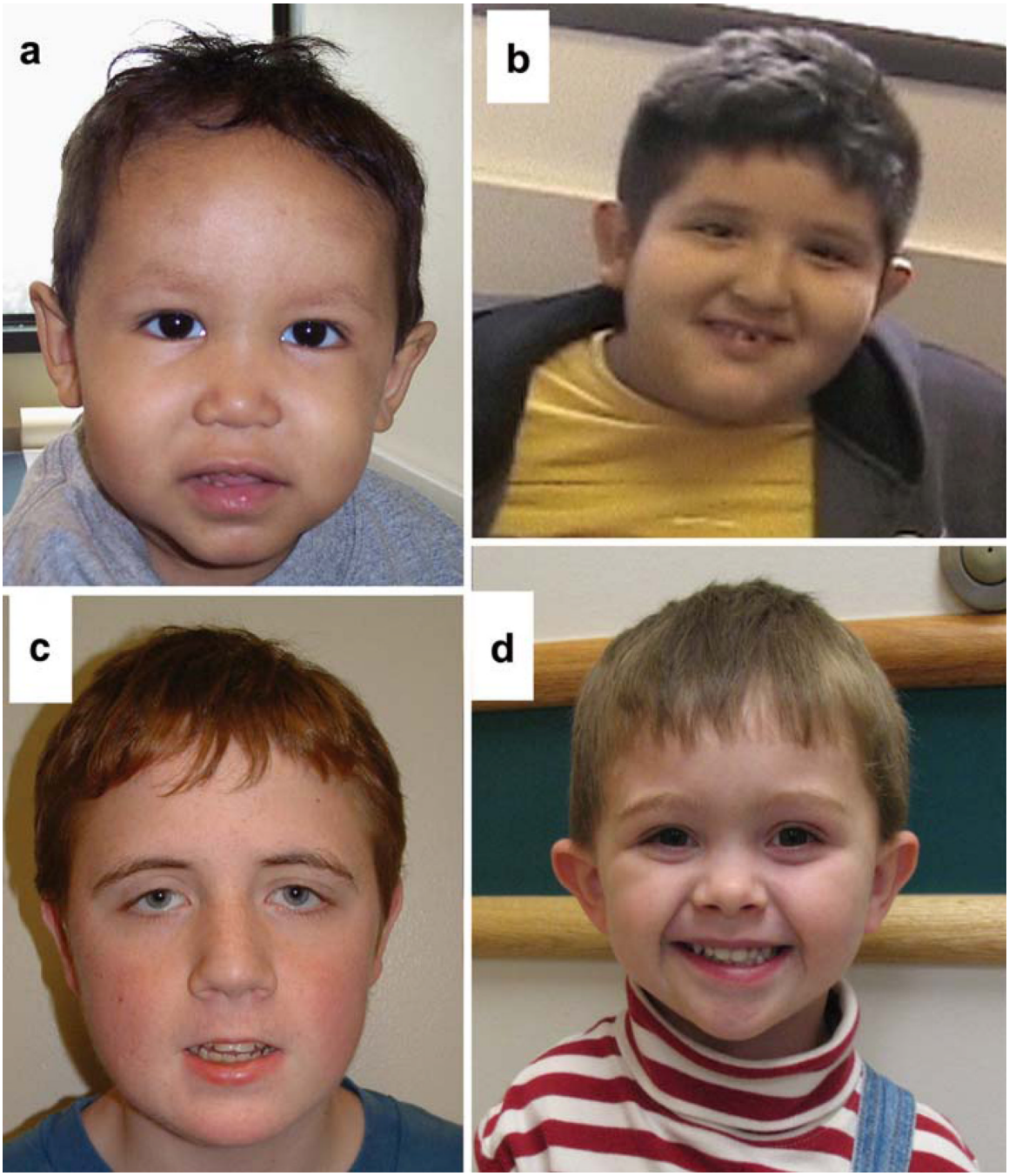

Fig. 2.

a Patient 1: Facial features, including high anterior hair line, broad forehead, sparse eye brows, epicanthal fold, depressed nasal bridge, long smooth philtrum, and full lower lip. **b** Patient 4: Facial features, including round face, facial asymmetry with left-sided smaller, cup-shaped protruding ears, and smooth philtrum. **c** Patient 5: Facial features, including long face, epicanthal folds, down-slanting palpebral fissures, ptosis, full puffy hooded eyelids, high nasal bridge, smooth philtrum, thin upper lip, and full lower lip. **d** Patient 6: Facial features, including rounded face, hypertelorism, flattened nasal bridge, and prominent ears

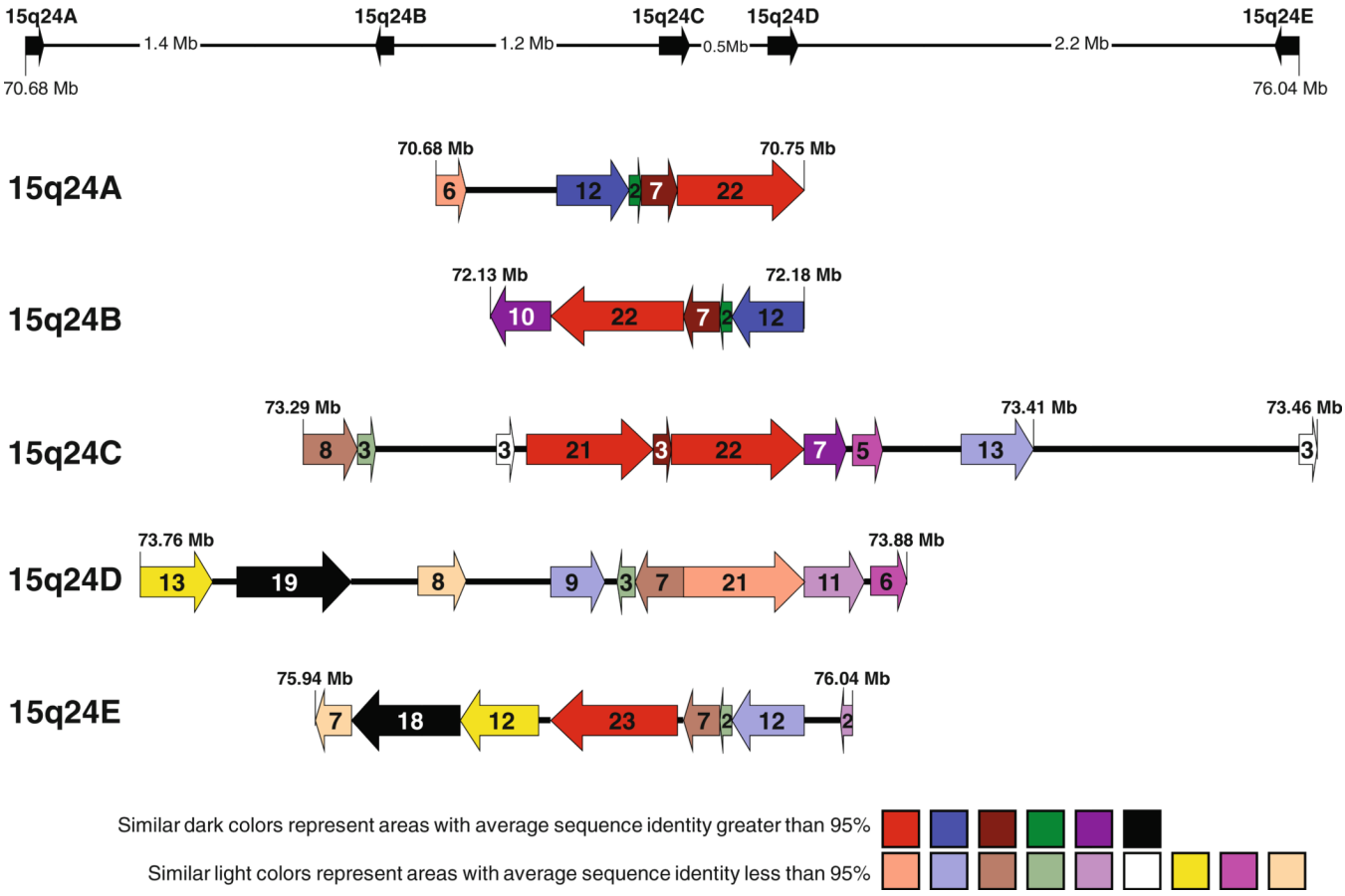

Fig. 3.

Summary of the results of the computational analysis of the genomic architecture in 15q24. The five LCR clusters: ~65 kb LCR14q24A (70.685–70.750 Mb), ~54kb LCR14q24B (72.134–72.188 Mb), ~124 kb LCR14q24C (73.295–73.419 Mb), ~128kb LCR14q24D (73.760–73.888 Mb), and ~93 kb LCR15q24E (75.948–76.041 Mb). LCRs subunits with sequence identity greater than 90% are shown as *arrows* with similar colors. The subunits with sequence identity more than 95% are represented in *darker colors* (e.g. *red*), whereas, the subunits with sequence identity between 90 and 94% are shown in *lighter colors* (e.g. *light red*). *Arrowheads* indicate LCR subunits orientation. The *numbers* inside the arrow represent the length of the area in kb

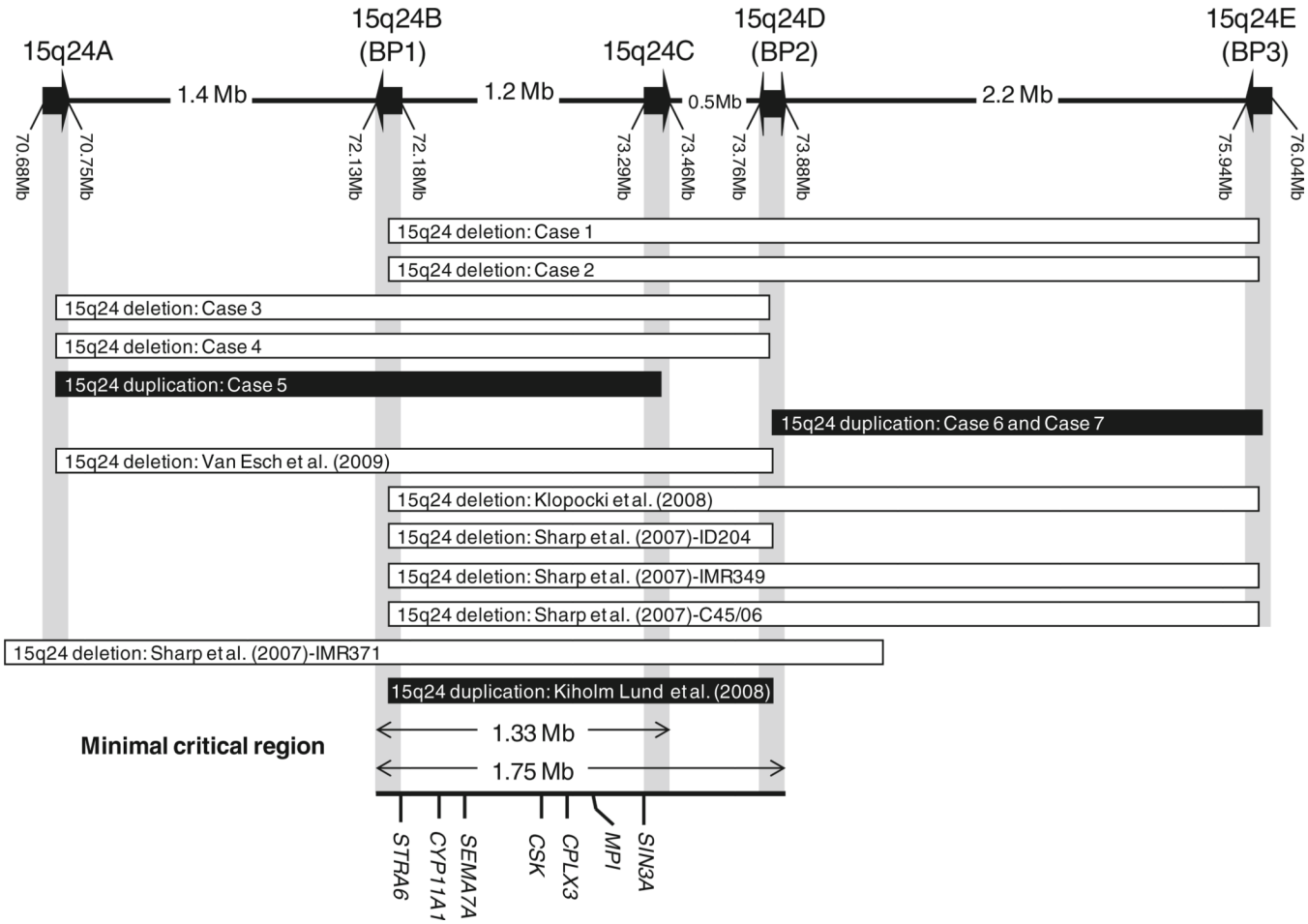

Fig. 4.

Schematic of the deleted/duplicated regions in chromosome 15q24: Case 1 (15q24del: 72.252–75.937 Mb), Case 2 (15q24del: 72.130–76.080 Mb), Case 3 (15q24del: 70.750–73.856 Mb), Case 4 (15q24del: 70.708–73.856 Mb), Case 5 (15q24dup: 70.708–73.332 Mb), and Cases 6 and 7 (15q24dup: 73.858–75.969 Mb), and the previously cases reported by Sharp et al. (2007), ID204 (15q24del: 72.15–73.85 Mb), IMR349 (15q24del: 72.15–76.01 Mb), C45/06 (15q24del: 72.15–76.01 Mb), and IMR371 (15q24del: 70.40–74.21 Mb), Klopocki et al. (2008), (15q24del: 72.2–75.9 Mb), Van Esch et al. (2009) (15q24del: 70.6–73.7 Mb), and Kiholm Lund et al. (2008) (15q24dup: 72.14–73.85 Mb). The LCRs are represented as *arrows*, LCR15q24A, LCR15q24B, LCR15q24C, LCR15q24D, and LCR15q24E. The minimal critical deletion region of ~1.75 Mb extends between LCR15q24B and LCR15q24D (72.134–73.888 kb) and the suggested minimal critical region for 15q24 duplication of ~1.33 Mb extending from LCR15q24B to LCR15q24C (72.134–73.419 kb). Selected genes in this region are shown: *STRA6, CYP11A1, SEMA7A, CSK, CPLX3, MPI*, and *SIN3A*

Table 1

The deleted regions and the clinical manifestations in patients with the 15q24 deletion

	Case 1	Case 2	Case 3	Case 4	Van Esch et al. (2009)	Klopocki et al. (2008)	Sharp et al. (2007) IMR349	Sharp et al. (2007) C45/06	Sharp et al. (2007) ID204	Sharp et al. (2007) IMR371
del 15q24 (length)	72.252–75.937 Mb (3.686 Mb)	72.130–76.080 Mb (3.950 Mb)	70.750–73.856 Mb (3.106 Mb)	70.708–73.856 Mb (3.148 Mb)	70.6–73.7 Mb (3.1 Mb)	72.2–75.9 Mb (3.7 Mb)	72.15–76.01 Mb (3.86 Mb)	72.15–76.01 Mb (3.86 Mb)	72.15–73.85 Mb (1.7 Mb)	70.40–74.21 Mb (3.72 Mb)
Inheritance	De novo	Unknown	De novo	De novo	De novo	De novo	De novo	De novo	Unknown	De novo
Age and gender	33 months	5 months	14 years	9 years	33 years	10 years	14 years	14 years	33 years	15 years
	Male	Female	Male	Male	Male	Male	Male	Male	Male	Male
Growth	Short stature	Short stature	Normal growth	Obesity	Obese Macrocephaly	Obesity	Short stature Microcephaly IUGR	Short stature Microcephaly IUGR	Short stature Microcephaly IUGR	Normal growth
Development	Mild delay	MR	Delayed	Moderate MR	Severe MR	Mild MR	Mild MR	Mild MR	Mild MR	Mild MR
Face	High anterior hair line	Frontal bossing	Normal appearance	Asymmetry	High anterior hair line	High anterior hair line	High anterior hair line	High anterior hair line	High anterior hair line	High anterior hair line
	Broad forehead	Brachycephaly		Round face	Long face		Long narrow face	Asymmetry	Asymmetry	Asymmetry
					Small maxilla large mandible			Happy facial expression	Happy facial expression	Happy facial expression
										Long narrow face
Eye	Sparse eye brows			Normal appearance	Broad medial eyebrows	Broad medial eyebrows	Broad medial eyebrows	Broad medial eyebrows	Broad medial eyebrows	Broad medial eyebrows
		Hypertelorism			Hypertelorism		Hypertelorism	Hypertelorism	Hypertelorism	Hypertelorism
			Down-slanting palpebral fissures		Down-slanting palpebral fissures	Down-slanting palpebral fissures	Down-slanting palpebral fissures	Down-slanting palpebral fissures	Down-slanting palpebral fissures	
	Epicanthus	Epicanthus	Epicanthus		Strabismus	Strabismus		Strabismus	Strabismus Epicanthus	
Nose	Depressed nasal bridge	Broad upturned nasal tip	Normal appearance	Normal appearance	Broad nasal base	Hypoplastic nostrils	Broad nasal base	Broad nasal base	Small nose	Broad nasal base
							Flaring alae nasi	Flaring alae nasi	Hypoplastic alae nasi	Flaring alae nasi
Mouth	Long smooth philtrum	Small mouth	Small mouth	Smooth philtrum	Long smooth philtrum	Long smooth philtrum	Long philtrum	Long smooth philtrum	Long smooth philtrum	Long philtrum
	Full lower lip				High palate		Full lower lip	Full lower lip	Full lower lip	Full lower lip
					Bifid uvula					
Ear	Ear lobe pit	Normal appearance	Thick, small ears	Cup-shaped protruding ears	Large ears	NA	Ear abnormalities	Ear abnormalities	Small everted ears	Hearing loss
			Ear lobe pit				Hearing loss			
Nervous system	Hypotonia	Myelomeningocele Hydrocephalus	Hypotonia	Hypotonia	Hypotonia	Hypotonia	Wide basal cisterna on brain MRI	Hypotonia	NA	NA
								Dysplastic corpus callosum on brain MRI	NA	NA
								Seizure		
Genital	Normal	Normal	Hypospadias	Microphallus	Microphallus Cryptorchidism	Microphallus	Normal	Hypospadias	Hypospadias	Hypospadias
Skeletal	No abnormalities	Clubfeet	Joint laxity	Joint laxity	Scoliosis	Joint laxity	Joint laxity	Scoliosis	Joint laxity	Joint laxity
			Pectus carinatum	Pes planus	Clubfeet	Lumbar lordosis	Scoliosis			Narrow chest

	Case 1	Case 2	Case 3	Case 4	Van Esch et al. (2009)	Klopocki et al. (2008)	Sharp et al. (2007) IMR349	Sharp et al. (2007) C45/06	Sharp et al. (2007) ID204	Sharp et al. (2007) IMR371
						Genua valga				Pes cavus
Digital anomalies	Small hands	Overriding second toes	Long first toes and short second toes	Brachymesopalangy II and V	Long slender fingers with distal tapering	Broad thumb	Long slender fingers	Proximally implanted thumbs	Small hands	Hypoplastic right thumb
		Clinodactyly		Clinodactyly		Brachydactyly	Proximally implanted thumbs		Brachydactyly	Contractures of fingers
						Clinodactyly				
Respiratory	No symptoms	No symptoms	Recurrent ear infections	Recurrent ear infections	High pitched voice	Nasal speech	Recurrent ear infections	Low tone voice	Recurrent upper airway infections	Recurrent chest infections
			Velo-pharyngeal insufficiency			Hoarse voice				Asthma
			Soft nasal speech			Clinodactyly				
Other	Acute lymphoblastic leukemia	Tetralogy of Fallot	Café au lait spots	Aggressiveness	Hyperactivity Aggressiveness	Inguinal and umbilical hernia	Attention deficit hyperactivity disorder	Edema of extremities	Feeding difficulties as child	Diaphragmatic hernia
	Feeding difficulties		Feeding difficulties	Cafe-au-lait spots	Diaphragmatic hernia	Skin laxity	Autistic features	GH deficiency		Inguinal hernia
	Hepatomegaly			Acanthosis nigricans	Inguinal hernia	Splenomegaly	GH deficiency	Hypogonado-tropic hypogonadism		
							Delayed puberty Bowel atresia	Bowel atresia		

NA not reported, *MR* mental retardation, *IUGR* intrauterine growth restriction

Table 2

The duplicated regions with the clinical manifestations in patients with the 15q24 duplication and the summary of the clinical features of the 10 patients with the 15q24 deletion

	15q24 deletion	15q24 duplications involving the minimal deletion critical region		15q24 duplications not involving the minimal critical region	
		Case 5	Kiholm Lund et al. (2008)	Case 6	Case 7
Dup 15q24 (length)		70.708–73.332 Mb (2.62 Mb)	72.15–73.85 Mb (1.7 Mb)	73.858–75.969 Mb (2.11 Mb)	73.858–75.969 Mb (2.11 Mb)
Inheritance		Unknown	Inherited from the father	Inherited from the mother	Inherited from the mother
Age and gender		15 years, male	2 years, male	3.5 years, male	2 years, female
Growth					
Short stature	5/10	Short stature	Normal growth	Normal growth	Normal growth
Microcephaly	3/10	–	–	–	–
IUGR	3/10	–	–	–	–
Obesity	3/10	–	–	–	–
Development delay	10/10	Mild MR	Delayed	Mildly delayed	Mildly delayed
Face					
High anterior hair line	7/10	–	Normal appearance	–	–
Facial asymmetry	4/10	–	–	–	–
Long face	3/10	Long face	–	Round face Flat occiput Plagiocephaly	Round face
Eye					
Broad medial eyebrows	6/10	–	–	–	–
Down-slanting palpebral fissures	6/10	Down-slanting palpebral fissures	Down-slanting palpebral fissures	–	–
Hypertelorism	6/10	–	Hypertelorism	Hypertelorism	Hypertelorism
Epicanthus	4/10	Epicanthus	Epicanthus	–	Epicanthus
		Full puffy hooded eyelids			
Strabismus	4/10	–	Strabismus	–	–
		Ptosis	Thick upper eyelid		
			High arched eyebrows		
Nose					
Broad nasal base	4/10	High nasal base	Broad nasal bridge	Flat nasal bridge	Normal appearance
Mouth					

	15q24 deletion	15q24 duplications involving the minimal deletion critical region		15q24 duplications not involving the minimal critical region	
		Case 5	Kiholm Lund et al. (2008)	Case 6	Case 7
Long/smooth philtrum	8/10	Smooth philtrum	Smooth philtrum	Normal appearance	Normal appearance
Full lower lip	5/10	Full lower lip High arched palate Crowded teeth Retrognathia	Full lower lip Triangular mouth		
Ear					
Malformation	7/10	Normal appearance	Low set posteriorly rotated ears	Prominent ears	Prominent ears
				Ear tag	
Nervous system					
Hypotonia	6/10	Hypertonia	Hypertonia	Truncal hypotonia	Truncal hypotonia
			Agenesis of corpus callosum on brain MRI	Lower extremities hypertonia	
Genital	7/10	Normal	Hypospadias	Normal	Normal
Skeletal					
Joint laxity	6/10	Decreased joint range of motion	Joint contractures	No abnormalities	No abnormalities
Digital	10/10	Broad thumbs	Overlapping fingers	Tapering fingers	Tapering fingers
		Blunt finger tips	Overlapping fingers		
		Hyperconvex nails	Hypoplastic nails		
		Broad feet	Broad finger pads		
Other		Attention deficit hyperactivity disorder	Oligohydramnios	Recurrent sinusitis, bronchitis, and otitis	Gastro-esophageal disease
		Asperger syndrome	Low posterior hairline		

Hum Genet. Author manuscript; available in PMC 2013 June 03.

Table 3

The coordinates, length, and orientation of LCR subunits for the five LCR clusters, LCR15q24A, LCR15q24B, LCR15q24C, LCR15q24D, and LCR15q24E

	Start	End	Length (kb)	Orientation	Subunit color
LCR14q24A	70,685,541	70,691,956	6,415	+	Light red
	70,707,347	70,719,598	12,251	+	Blue
	70,719,670	70,721,200	1,530	+	Green
	70,721,201	70,728,580	7,379	+	Brown
	70,729,074	70,750,593	21,519	+	Red
LCR14q24B	72,134,535	72,144,840	10,305	−	Violet
	72145146	72,166,963	21,817	−	Red
	72,167,460	72,174,829	7,369	−	Brown
	72,174,830	72,176,359	1,529	−	Green
	72,176,431	72,188,813	12,382	−	Blue
LCR14q24C	73,295,360	73,303,732	8,372	+	Light brown
	73,304,189	73,307,393	3,204	+	Light green
	73,328,277	73,330,953	2,676	+	White
	73,332,931	73,354,116	21,185	+	Red
	73,354,117	73,356,715	2,598	+	Brown
	73,357,211	73,378,995	21,784	+	Red
	73,379,350	73,386,517	7,167	+	Violet
	73,387,968	73,393,463	5,495	+	Pink
	73,406,153	73,418,809	12,656	+	Light blue
	73,463,299	73,466,244	2,945	+	White
LCR14q24D	73,760,220	73,772,788	12,568	+	Yellow
	73,777,284	73,796,657	19,373	+	Black
	73,807,737	73,815,337	7,600	+	Tan
	73,828,848	73,838,186	9,338	+	Light blue
	73,839,617	73,842,915	3,298	−	Light green
	73,842,941	73,849,886	6,945	−	Light brown
	73,849,902	73,870,477	20,575	+	Light red

	Start	End	Length (kb)	Orientation	Subunit color
LCR14q24E	73,870,478	73,881,040	10,562	+	Light purple
	73,882,218	73,888,387	6,169	+	Pink
	75,948,172	75,954,860	6,688	–	Tan
	75,955,173	75,973,569	18,396	–	Black
	75,973,925	75,985,550	11,625	–	Yellow
	75,987,909	76,011,121	23,212	–	Red
	76,011,796	76,019,176	7,380	–	Light brown
	76,019,184	76,020,691	1,507	–	Light green
	76,020,763	76,033,111	12,348	–	Light blue
	76,039,907	76,041,935	2,028	–	Light violet